

# Technical Notes

*TECHNICAL NOTES are short manuscripts describing new developments or important results of a preliminary nature. These Notes cannot exceed 6 manuscript pages and 3 figures; a page of text may be substituted for a figure and vice versa. After informal review by the editors, they may be published within a few months of the date of receipt. Style requirements are the same as for regular contributions (see inside back cover).*

## Comparison of Optimization Algorithms for Aerodynamic Shape Design

Shigeru Obayashi\* and Takanori Tsukahara†  
Tohoku University, Sendai 980-77, Japan

### Introduction

**A**ERODYNAMIC shape optimization is one of the major research areas of the present computational fluid dynamics community.<sup>1</sup> Although various techniques have been presented, they have usually concentrated on how the existing optimization algorithms are applied to aerodynamic problems. There were few papers that assessed performance of the optimization algorithms for aerodynamic problems.

In this Note, three different optimization algorithms are applied to airfoil design. A simplified test problem is considered here so that the distribution of the objective function can be plotted. The visualization of the objective function will reveal which optimization strategy is preferable. The results of three optimization algorithms will be easy to compare and to evaluate as to performance.

One of the three algorithms employed here is the gradient-based method (GM).<sup>2</sup> In this method, the design is updated iteratively in the direction of the steepest ascent from the initial design (the hill-climbing strategy). Many variations of GM have been used widely inasmuch as the optimum obtained from GM is a global optimum if the objective and constraints are differentiable and convex.<sup>2</sup> In practice, however, it is very difficult to prove these properties. One could only hope for a local optimum in the neighborhood of the initial point, provided that the gradient is well defined. Therefore, one must start the design from various initial points to determine if a consistent optimum can be obtained while having reasonable assurance that this is the true optimum.

The second is the method of simulated annealing (SA).<sup>3</sup> SA is a heuristic strategy for obtaining near-optimal solutions and derives its name from an analogy to the annealing of solids. Basically, in this method, the design is updated if a randomly disturbed one is better. This strategy is still hill climbing, and it could end up with local extrema easily as GM does. Thus, SA also accepts a poorer design with certain probability related to the Boltzmann distribution under the specified annealing schedule. Therefore, there is a corresponding chance for the design to get out of a local extreme in favor of finding a better, more global one.

The last of the three is genetic algorithm (GA).<sup>4</sup> GA is a search algorithm based on the mechanics of natural selection and natural genetics. GA searches an optimum through simulated evolution. During evolution, genotypes (design variables) producing phenotypes (designs) of increasing biological fitness (objective function)

are created by means of mutation and recombination of genotypes and by selection of phenotypes. The combination of mutation and recombination, in principle, allows for leaving a smaller hill and, therefore, prevents evolution from getting stuck on local extrema.

Recently, GA has attracted attention as a robust optimization tool.<sup>5,6</sup> However, because GA requires a large number of function evaluations, one might question why GA is preferred against other methods. The aim of this Note is to answer this question and demonstrate GA's ability using a simplified optimization problem.

### Airfoil Design Using Approximation Concept

Aerodynamic design of airfoils is considered. The purpose is to determine the contour  $y$  for both upper and lower surfaces at every chordwise location. How the  $y$  coordinate is defined determines the choice of design variables. The design variables can be pointwise values of the  $y$  coordinates, arbitrary functions, a base airfoil shape with perturbation functions, or a combination of the existing airfoil shapes.

Following Ref. 2, we define  $\mathbf{Y}^1, \mathbf{Y}^2, \dots, \mathbf{Y}^N$  as vectors containing the coordinates of the airfoil's upper surface followed by those of the lower surface at given chordwise locations. They are basis vectors, corresponding to the existing airfoil shapes. Thus, an airfoil shape is defined as

$$\mathbf{Y} = a_1 \mathbf{Y}^1 + a_2 \mathbf{Y}^2 + \dots + a_N \mathbf{Y}^N \quad (1)$$

The design variables are now  $a_1 - a_N$ . Thus, the number of design variables is greatly reduced compared to having pointwise values of the  $y$  coordinates over 50 chordwise locations. In the following, four basis airfoil shapes are used ( $N = 4$ ). As defined in Ref. 2,  $\mathbf{Y}^1, \mathbf{Y}^2, \mathbf{Y}^3$ , and  $\mathbf{Y}^4$  indicate NACA2412, NACA64<sub>1</sub>-412, NACA65<sub>2</sub>-415, and NACA64<sub>2</sub>A215, respectively.

### Results and Discussions

To simplify the present aerodynamic problem, low-speed airfoils are considered, assuming that the flowfield is governed by the two-dimensional, incompressible, inviscid flow equation. A simple panel method can be used for the flow analysis.<sup>7</sup>

Now let us consider the lift maximization problem. The objective function to be maximized is thus defined as the lift coefficient. The only constraint used is that the maximum airfoil thickness is to be 15% of the chord. The angle of attack is fixed at 6 deg.

The first test case considers lift maximization with two design variables,  $a_1$  for NACA2414 and  $a_2$  for NACA64<sub>1</sub>-412, for demonstration purposes. Because only two design variables are used, we can easily visualize the distribution of the objective function  $C_l$  as shown in Fig. 1, where  $-5 < a_1, a_2 < 5$ , and the lift coefficients are computed at an interval of 0.2 for both  $a_1$  and  $a_2$  coordinates. The negative value of the lift is replaced by zero.

The resulting distribution of the aerodynamic performance is highly irregular. Because the flow equation is linearized and only two design variables are involved, one might expect a smooth distribution of the objective function. When both design variables are positive, the lift variation is smooth as expected. In fact, Fig. 1 indicates that the maximum lift is achieved when  $a_1 = a_2 = 5$ . However, it is not acceptable because the airfoil thickness will be about 120% of the chord. When one of the design variables becomes negative, the resulting lift distribution tends to have sharp, distinct, multiple peaks. This is because the upper surface may crisscross the lower surface. This is a typical situation where GM does not work.

Presented as Paper 96-2394 at the 14th AIAA Applied Aerodynamics Conference, New Orleans, LA, June 17–20, 1996; received Aug. 29, 1996; revision received April 14, 1997; accepted for publication April 23, 1997. Copyright © 1997 by the American Institute of Aeronautics and Astronautics, Inc. All rights reserved.

\*Associate Professor, Department of Aeronautics and Space Engineering. E-mail: obayashi@ad.mech.tohoku.ac.jp. Senior Member AIAA.

†Graduate Student, Department of Aeronautics and Space Engineering.

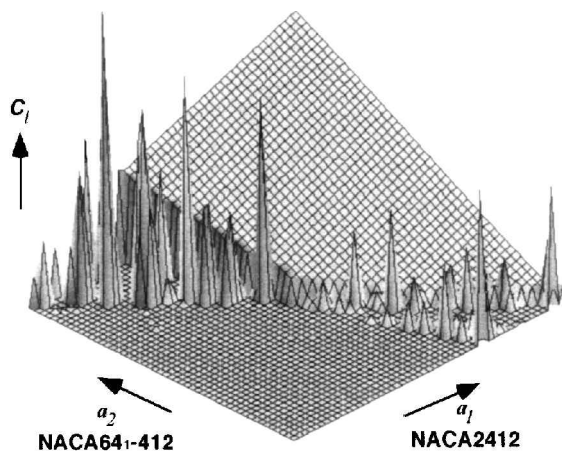


Fig. 1 Lift distribution of the first test case.

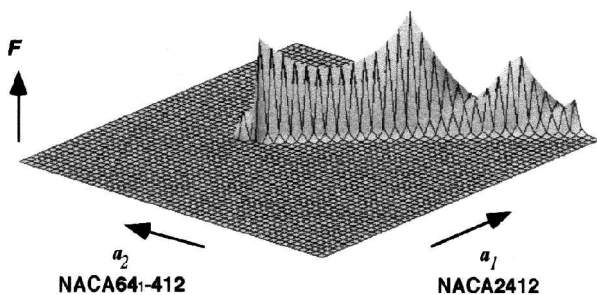


Fig. 2 Objective function distribution, lift coefficient with a penalty for airfoil thickness.

To see the effect of the constraint as a penalty, the objective function is now redefined by using a penalty function with the airfoil thickness  $t/c$  as

$$F = C_l \cdot \exp[-100 \times (t/c - 0.15)] \quad (2)$$

The corresponding function distribution is shown in Fig. 2. Although distinct, multiple peaks are greatly reduced, most of the design space now has zeros or negative objective function values. The design space with positive objective function values is found only in the narrow ridge where the constraint is satisfied, and it still contains five local extrema. This is another typical situation where GM has difficulty.

Figure 2 also suggests that the design variables are improperly defined. However, this is realized only after the distribution of the objective function is calculated. The task of optimization is to find an optimum without computing a global distribution of objective functions. Inasmuch as aerodynamic function behaves unexpectedly even in this simplified problem, a certain mechanism to locate a global optimum is required. The combination of mutation and recombination of GA will be effective to find an optimal solution. On the other hand, a simple hill-climbing strategy requires the initial design to be very close to the optimum. Thus, the hill-climbing strategy is practically inapplicable to these kinds of problems.

The second test case considers the lift maximization with a full set of four design variables. This time, the three optimization methods were actually run for comparison. The same constraint and flow condition were used. Figure 3 summarizes convergence history of the optimum lift values obtained from all three methods.

For GM, ADS V3.0, a Fortran program for automated design synthesis, was used.<sup>8</sup> Among the options of the code, the feasible direction method was used. The gradient information was given by the finite difference method. From the preceding test case, it is obvious that performance of GM will depend on the initial guess. Thus, the four apparent initial designs were used for the optimization:  $(a_1, a_2, a_3, a_4) = (1, 0, 0, 0), (0, 1, 0, 0), (0, 0, 1, 0),$  and  $(0, 0, 0, 1)$ . These four runs gave four different results. The best result shown in Fig. 3 [from the second set of the initial values,  $(0, 1, 0, 0)$ ] indicates the maximum lift coefficient of 1.716 at 159 function evaluations, whereas the worst run [the third set,  $(0, 0, 1, 0)$ ]

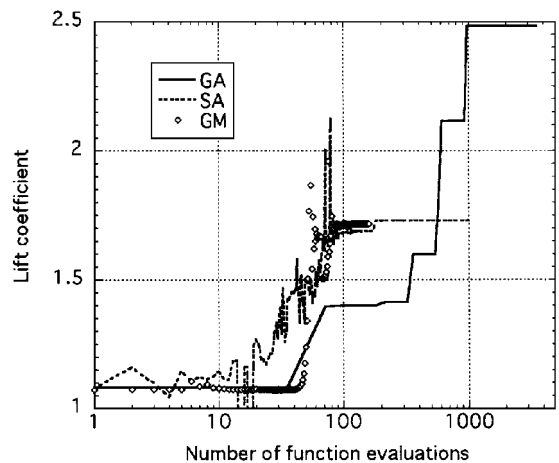


Fig. 3 Comparison of optimization histories among GM, SA, and GA.

does not allow the computation to continue after reaching negative thickness of the airfoil.

For SA, the algorithm combined with the downhill simplex method (as described in Ref. 3), is used. The cooling schedule was decided on the basis of trial and error so that the optimization problem was computed within a reasonable time. Because all four runs found some local maxima starting from the same initial designs as the GM case, SA is more robust than GM. However, like GM, it gave four different results. The best result [shown in Fig. 3 (from the third set)] gave the lift coefficient of 1.728 at 217 iterations, which is slightly better than the result of the GM case.

For GA, the simple GA in Ref. 4 is adapted for the real number coding of the design variables. One design variable is represented by two real numbers,  $r_1$  and  $r_2$ , for example,

$$a_1 = 0.65 \cdot r_1 + 0.35 \cdot r_2 \quad (3)$$

A simple roulette wheel selection operator is used here with a linear fitness scaling. The crossover operator exchanges the real numbers  $r_1$  and  $r_2$  for each design variable at probability of 0.5. The mutation operator adds a uniform random number between  $-0.1$  and  $+0.1$  to the real numbers  $r_1$  and  $r_2$  at probability of 0.2. There is no particular initial design here, but the initial population was created by assigning three uniform random numbers in an interval from  $-5$  to  $+5$  to  $a_1, a_2,$  and  $a_3$  and by calculating  $a_4 = 1 - a_1 - a_2 - a_3$ . In this run, we used 36 members for the population. After 27 generations, the optimal design was found. This corresponds to 972 function evaluations, roughly six times of the GM case.

The lift coefficient of the GA case is 2.480, which is the best of the three and much higher than those of the GM and SA cases. Although both GA and SA are capable of getting out of local extrema, GA outperforms SA. This is because GA searches an optimum in parallel from a population, whereas SA allows only a single perturbation at each step. Thus, the result of GA depends on the initial design less than that of SA.

The comparison of number of function evaluations required for the three methods indicates that GA is the most time consuming. However, if we use GM or SA, we would have to run it starting from many different initial designs to obtain a comparable result. Because there are no guidelines on properly choosing the initial design, an exhaustive, random search must be performed. Or, if we sample five initial designs evenly from each design variable, then we would need 20 trial runs for the present case. As a result, GM and SA will not have any advantage in efficiency. Overall, GA is the best choice for this test case.

In general, aerodynamic performance is sensitive to geometries. So far, any theory of fluid dynamics cannot tell us how to choose design variables that will guarantee the convexness of the objective function. In compressible flows, the objective function itself may be discontinuous due to shock waves. Thus, the distribution of the objective function will be quite unexpected and the resulting aerodynamic optimization problem will be very difficult. In this situation, a global search algorithm is indispensable and, thus, GA is preferred for the aerodynamic optimization.

## References

- <sup>1</sup>Dolling, D. S., and Grossman, B. (eds.), "CFD in Design," AIAA 12th Computational Fluid Dynamics Conf., San Diego, CA, June 1995.
- <sup>2</sup>Vanderplaats, G. N., *Numerical Optimization Techniques for Engineering Design: With Applications*, McGraw-Hill, New York, 1984, pp. 153–226.
- <sup>3</sup>Press, W. H., Teukolsky, S. A., Vetterling, W. T., and Flannery, B. P., *Numerical Recipes in FORTRAN: The Art of Scientific Computing*, 2nd ed., Cambridge Univ. Press, Cambridge, England, UK, 1992, pp. 436–448.
- <sup>4</sup>Goldberg, D. E., *Genetic Algorithms in Search, Optimization and Machine Learning*, Addison-Wesley, Reading, MA, 1989, pp. 59–88.
- <sup>5</sup>Quagliarella, D., and Cioppa, A. D., "Genetic Algorithms Applied to the Aerodynamic Design of Transonic Airfoils," *Journal of Aircraft*, Vol. 32, No. 4, 1995, pp. 889–891.
- <sup>6</sup>Doorly, D., "Parallel Genetic Algorithms for Optimization in CFD," *Genetic Algorithms in Engineering and Computer Science*, edited by G. Winter, J. Periaux, M. Galán, and P. Cuesta, Wiley, Chichester, England, UK, 1995, pp. 251–270.
- <sup>7</sup>Katz, J., and Plotkin, A., *Low-Speed Aerodynamics: From Wing Theory to Panel Methods*, International ed., McGraw-Hill, New York, 1991, pp. 301–377.
- <sup>8</sup>Vanderplaats, G. N., "ADS—A FORTRAN Program for Automated Design Synthesis, Version 3.00," Engineering Design Optimization, Inc., Santa Barbara, CA, March 1988.

A. Plotkin  
Associate Editor

# Suitability of Upwind-Biased Finite Difference Schemes for Large-Eddy Simulation of Turbulent Flows

Rajat Mittal\* and Parviz Moin†  
Stanford University, Stanford, California 94305

## Introduction

LARGE-EDDY simulation (LES) with the dynamic model<sup>1,2</sup> produces good results when used in conjunction with spectral-method-based solvers.<sup>3</sup> The dynamic modeling procedure utilizes information from the small scales of the flowfield, which are typically not corrupted by numerical errors in spectral simulations. However, spectral methods are usually limited to simple geometries, and for complex configurations, conventional finite difference methods are used. A fifth-order one-point upwind-biased scheme has been successfully used in well-resolved direct numerical simulations of turbulent flows,<sup>4</sup> and it was thought that the high resolving power and relatively low numerical dissipation of such a scheme would make them useful in LES of flows in complex geometries. To study the utility of these schemes for LES, Beaudan and Moin<sup>5</sup> employed them in a series of simulations of flow past a circular cylinder at  $Re = 3.9 \times 10^3$ , where the Reynolds number is based on the diameter  $D$  and freestream velocity  $U_\infty$ . This is a challenging flow for the LES methodology because it contains features such as thin laminar boundary layers, unsteady separation, and transitional shear layers. The particular Reynolds number was chosen owing to the availability of two experimental data sets. Lourenco and Shih used a particle image velocimetry technique to measure turbulence statistics in the near-wake region including the recirculation zone. Ong and Wallace<sup>6</sup> used a hot-wire probe for measuring mean velocity and stress profiles in the downstream wake region from  $x/D = 3$  to 10.

Beaudan and Moin<sup>5</sup> carried out simulations with no subgrid-scale (SGS) model, with a fixed coefficient Smagorinsky model, and with

the spanwise averaged version of the dynamic model<sup>1,2</sup> and observed that mean wall statistics such as drag, wall pressure coefficient, wall shear stress, and separation angles were not significantly different in the three simulations and all showed reasonable agreement with experimental data. The most significant finding of these simulations came from the comparison of the computed solution with the experiments in the region downstream of the vortex formation region ( $5.0 < x/D < 10.0$ ) where the mesh was relatively coarse. It was found that, in this region, numerical dissipation overwhelmed the contribution of the SGS model, and the three computed solutions were virtually indistinguishable beyond  $x/D > 7.0$ . The simulation with a seven-order scheme also showed that energy in a substantial portion of the resolvable wave number range was damped due to numerical dissipation, and it was concluded that these high-order upwind-biased schemes were unsuitable for use in LES.

Analysis of the truncation error<sup>5</sup> indicates that higher-order upwind-biased schemes provide good resolution in about two-thirds of the wave number range, and the upper-half of the wave number range is affected by numerical dissipation. In contrast to upwind-biased schemes, which control aliasing errors through numerical dissipation, in central schemes aliasing must be controlled by enforcing kinetic energy conservation. Such schemes do not exhibit numerical dissipation and, therefore, there is no spurious damping of the smaller scales. This feature makes the schemes attractive for use in LES, and a number of complex flows have been successfully simulated using a second-order central difference scheme on a staggered mesh.<sup>7,8</sup> One disadvantage of using these schemes is the dominance of dispersive error, which makes them extremely sensitive to aspects such as the grid stretching factors and outflow boundary conditions. These issues apparently do not present difficulties in simulations of relatively simple flows such as channel flow or flat plate boundary layers but are critical when simulating flows in complex geometries. Thus, even though the central schemes seem more attractive for LES, the advantage of these schemes over the higher-order upwind schemes for LES in complex flows needs to be established, and this is the main motivation for the current study.

We have simulated flow past a circular cylinder at a Reynolds number of  $3.9 \times 10^3$  using a solver that employs an energy-conservative second-order central difference scheme for spatial discretization. Detailed comparisons of turbulence statistics and energy spectra in the downstream wake region ( $7.0 < x/D < 10.0$ ) have been made with the results of Beaudan and Moin<sup>5</sup> and with experiments<sup>4</sup> to assess the impact of numerical diffusion on the flowfield. Based on these comparisons, conclusions are drawn on the suitability of higher-order upwind schemes for LES in complex geometries.

## Simulation Methodology

The solver used in the current work is based on the numerical scheme developed by Choi et al.,<sup>9</sup> which solves the incompressible Navier–Stokes equations in generalized coordinates on a spanwise periodic domain. The governing equations are written in terms of the volume fluxes, and the in-plane ( $x$ – $y$  plane) volume fluxes and pressure are discretized on a fully staggered grid using a second-order central difference scheme. The spanwise volume flux is collocated at the pressure node, and a Fourier spectral collocation method is used in the spanwise direction. Dealiasing is performed in the spanwise direction using a two-thirds truncation rule to make the numerical scheme energy conservative.

A C-mesh is used for the present simulation. The branch cut of the mesh is located along the wake centerline and the inflow and outflow boundaries are located at  $19D$  and  $17D$ , respectively. Furthermore, the vertical extent of the outflow boundary is about  $25D$  from the wake centerline. Uniform freestream velocity is prescribed at the inflow and far-field boundaries, and a convective boundary condition is employed at the outflow boundary to smoothly convect the disturbances out of the computational domain. The spanwise domain size  $L_z$  is chosen equal to  $\pi D$ , which is the same as that used by Beaudan and Moin.<sup>5</sup> It has been found that in LES, where the resolution is at best marginal, central schemes can tolerate only a small streamwise stretching factor ( $< 3\%$ ); higher stretching factors can lead to the amplification of grid-to-grid oscillations ( $2\Delta$  waves). If an O-type

Received Dec. 9, 1996; revision received April 16, 1997; accepted for publication April 30, 1997. Copyright © 1997 by the American Institute of Aeronautics and Astronautics, Inc. All rights reserved.

\*Research Fellow, Center for Turbulence Research; currently Assistant Professor, Department of Mechanical Engineering, University of Florida, Gainesville, FL 32611-6300.

†Director, Center for Turbulence Research.